Nuclear Magnetic Resonance Laboratory

Created by: *Anita Karsa, Dávid Iván, Gábor Csősz, Bence Gábor Márkus and Ferenc Simon*
December 2012, Updated: September 2024.(Robin Kucsera and Ferenc Simon)

Location of lab: Building F I. basement 2., Magnetooptics Laborarory.
Contacts: Robin Kucsera: kucsrobin@gmail.com, Simon Ferenc: simon.ferenc@ttk.bme.hu

1 Introduction

Nuclear Magnetic Resonance (NMR) spectroscopy was created over 80 years ago, that since has been applied in the fields of physics, chemistry, biology and medicine as well. In practice, it can be used to investigate superconductors, proteins' and other biomolecules' change in structure for pharmaceutical research, exploration of crude oil and medical imaging techniques. The aim of this lab is to introduce NMR spectroscopy and the usage of an NMR apparatus on a 300 MHz (7 T) equipment, that has been put into operation in 2012. During the lab, students will get a deeper understanding of the NMR circuitry and the build-up of the probeheads, then the measurements and pulse sequences.

2 Theoretical background

The idea behind NMR spectroscopy is that certain atomic nuclei possess magnetic moments. Although this is relatively weaker (approx. 1/1000th) compared to the magnetic moment of electrons, this collective magnetism of the nuclei can be manipulated and read out to get information on the density of the nuclei in a material or the environment of nuclei, the arrangement of neighbouring bonds, chemical configuration. Among these so-called NMR-active nuclei, the proton (^{1}H) stands out due to it having the strongest NMR signal and as it is the most common nucleus in living organisms, it has a great medical importance, as well. Additionally, in biological studies, we encounter NMR spectroscopy of nuclei such as ^{2}D, ^{13}C, ^{14}N, ^{15}N, ^{17}O, ^{19}F, ^{23}Na, ^{31}P, ^{35}Cl, ^{129}Xe, and ^{195}Pt.

The basis of atomic magnetism is that electrons, protons, and neutrons each have their own angular momentum (spin, S) to which a magnetic moment (μ) is coupled. In the case of electron, the coupling constant between these two quantities, the so-called *g factor* can be given by the equation $\mu = -g \cdot \mu_\mathrm{B} \cdot S$[1], and its value is generally around $g = 2$[2]. In the case of atomic nuclei, we speak of nuclear spin I, the value of which is determined by the filling of proton and neutron shells within the nucleus. The magnetic moment associated with a given nuclear spin I varies widely (by 2 orders of magnitude). The reason for this is that protons and neutrons are not elementary particles but are composed of quarks, making it necessary to describe the entire quark system to specify the value of the magnetic moment.

The magnetic moment of a classical current loop is equal to the product of the area and the current. Thus, the magnetic moment μ resulting from the motion of a charged particle in a circular orbit is:

$$\mu = A \cdot I = (r^2\pi) \cdot \left(\frac{qv}{2\pi r}\right) = \frac{qN}{2m},$$

where q is the charge of the particle, N is its angular momentum, and m is its mass. A particle with charge q and orbital angular momentum $\hbar L$ (where L is the orbital angular momentum quantum number) generates the following magnetic moment:

$$\mu = \frac{q\hbar L}{2m}.$$

For an electron, $m = m_e$ and $q = -e$, where e is the elementary charge. The electron has a magnetic moment originating from its intrinsic angular momentum, with a magnitude given by:

$$\mu_\mathrm{el} = -2\mu_\mathrm{B} S,$$

where the factor of 2 comes from the g-factor derived from the Dirac equation (see above), and S is the spin or intrinsic angular momentum.

Since protons and neutrons are not elementary particles, describing their magnetic moments requires considering their constituents, the quarks. The magnetic moments of atomic nuclei and nucleons are given in the so-called *nuclear magneton* units:

$$\mu_\mathrm{N} = \frac{e\hbar}{2M_\mathrm{p}} = 5.05 \cdot 10^{-27}\mathrm{Am}^2,$$

where M_p is the mass of the proton. According to the quark model, both the proton and neutron are composed of 3 quarks each. The proton consists of two up quarks (u) and one down quark (d), while the neutron consists of one up

[1] $\mu_\mathrm{B} = \frac{e\hbar}{2m_e} = 9.274 \cdot 10^{-24}\ \frac{\mathrm{J}}{\mathrm{T}}$ is the so-called *Bohr magneton*, the negative sign indicating the negative charge of the electron.
[2] The exact value is $g = 2.0023$ due to *quantum-electrodynamical* corrections.

quark and two down quarks. Since the up quark has a charge of $\frac{2}{3}e$, and the down quark has a charge of $-\frac{1}{3}e$, this gives the proton a charge of e, while the neutron is electrically neutral.

The magnetic moment of the proton can thus be traced back to that of the quarks:

$$\mu_{\mathrm{p}^+} = \frac{4}{3}\mu_{\mathrm{u}} - \frac{1}{3}\mu_{\mathrm{d}} = 2.79 \cdot \mu_{\mathrm{N}},$$

$$\mu_{\mathrm{n}^0} = \frac{2}{3}\mu_{\mathrm{d}} - \frac{2}{3}\mu_{\mathrm{u}} = -1.91 \cdot \mu_{\mathrm{N}}.$$

It is somewhat surprising that the neutral neutron also has a magnetic moment. In the case of atomic nuclei, the magnetic moment can also be expressed in the following form:

$$\mu = \gamma \cdot \hbar \cdot I.$$

Here, γ is the so-called *gyromagnetic ratio* (with dimensions of 1/sT). In practice, both the values of I and γ are obtained from tables for the nucleus to be studied. This is because even a simple system, such as ^{2}D, cannot be described merely as the sum of a proton and a neutron.

There are two possible methods to introduce the basis of NMR spectroscopy: 1) a phenomenological approach, where the collective magnetism of the nuclei is treated as a classical variable, and 2) a quantum mechanical approach, where the nuclear magnetism of individual nuclei is given as the eigenvalues of the Zeeman-Hamilton operator, and we consider their time evolution. It can be shown that the two descriptions are equivalent; however, the classical approach is technically easier and much more intuitive, so we will follow this approach here as well.

A magnetic dipole placed in a magnetic field experiences a torque, resulting in a so-called Larmor precession around the magnetic field, with an angular frequency: $\omega = \gamma \cdot B$. Here, B is the magnitude of the magnetic field, and γ is the (nucleus-dependent) gyromagnetic ratio, for example, for proton it is $\gamma(^1\mathrm{H}) = 2\pi \cdot 42.576$ MHz/T.

The magnetization (magnetic moment per unit volume) can be considered as a classical variable corresponding to the spins of atomic nuclei. The motion of this magnetization in a magnetic field is described by the so-called *Bloch equations* (1). The equations describe two qualitatively different processes. One is the rotation around the $\boldsymbol{M} \times \boldsymbol{B}$ axis, the other is the exponential relaxation present in all directions. In this description, the z-axis is chosen as the direction of the static magnetic field (with magnitude B_0) that forms the basis of the NMR apparatus. M_0 is the magnetization that develops after placing the sample in the magnetic field. This equilibrium magnetization is in the z direction, while the x-y components are zero.

T_1 and T_2 describe the relaxation times by which the magnetization vector relaxes to its equilibrium values in the z and the x-y direction, respectively. For historical reasons, T_1 and T_2 are called spin-lattice and spin-spin relaxation times, but they are also referred to as longitudinal and transverse relaxation times.

$$\begin{aligned}
\frac{\mathrm{d}M_z(t)}{\mathrm{d}t} &= \gamma \cdot (\boldsymbol{M}(t) \times \boldsymbol{B}(t))_z - \frac{M_z(t) - M_0}{T_1} \\
\frac{\mathrm{d}M_x(t)}{\mathrm{d}t} &= \gamma \cdot (\boldsymbol{M}(t) \times \boldsymbol{B}(t))_x - \frac{M_x(t)}{T_2} \\
\frac{\mathrm{d}M_y(t)}{\mathrm{d}t} &= \gamma \cdot (\boldsymbol{M}(t) \times \boldsymbol{B}(t))_y - \frac{M_y(t)}{T_2}
\end{aligned} \tag{1}$$

In NMR techniques, when the sample is placed in a homogeneous magnetic field that is a few Tesla in magnitude, the magnetic moments of atomic nuclei with intrinsic spin align with the direction of the field. To induce magnetic resonance, a much smaller magnetic field (B_1, with a magnitude of a few mT) is applied, which rotates at the Larmor frequency. The B_1 magnetic field also creates a torque on the nuclear spins, but its magnitude is much smaller than that of the B_0 field. However, since this magnetic field rotates in phase with the magnetization of the nuclear spins, the contributions of the B_1 torque add up and tilt the direction of the nuclear spins away from the equilibrium z-direction.

The B_1 magnetic field is generated by an alternating voltage with an angular frequency ω_{L} applied to an RF (radiofrequency) coil oriented in the x or y direction surrounding the sample. If, for example, the nuclear magnetization is rotated into the x-y plane by a suitably chosen B_1 pulse, the magnetization, while Larmor precessing, induces voltage in the coil, which can be detected. After the excitation, a much longer characteristic relaxation follows, the temporal decay of which can be tracked by the change in the amplitude of the voltage induced in the coil. Based on the voltage induced in the coil, the x and y components of the magnetic moment can be measured.

The process is most simply described in the X, Y, Z coordinate system, which rotates with the magnetization at the Larmor precession frequency (the laboratory system is the x, y, z system). In this system, the B_1 excitation field is most commonly aligned along the X or Y directions. It can be seen that in this system, the nuclear magnetization will undergo *Rabi precession* around the B_1 direction with an angular frequency of $\omega_R = \gamma \cdot B_1$. If the B_1 excitation is applied for some time τ, then the nuclear spin will ultimately precess by an angle of $\omega_{\mathrm{R}} \cdot \tau$ from its original position. The applied pulses during the measurement are characterized by this angle.

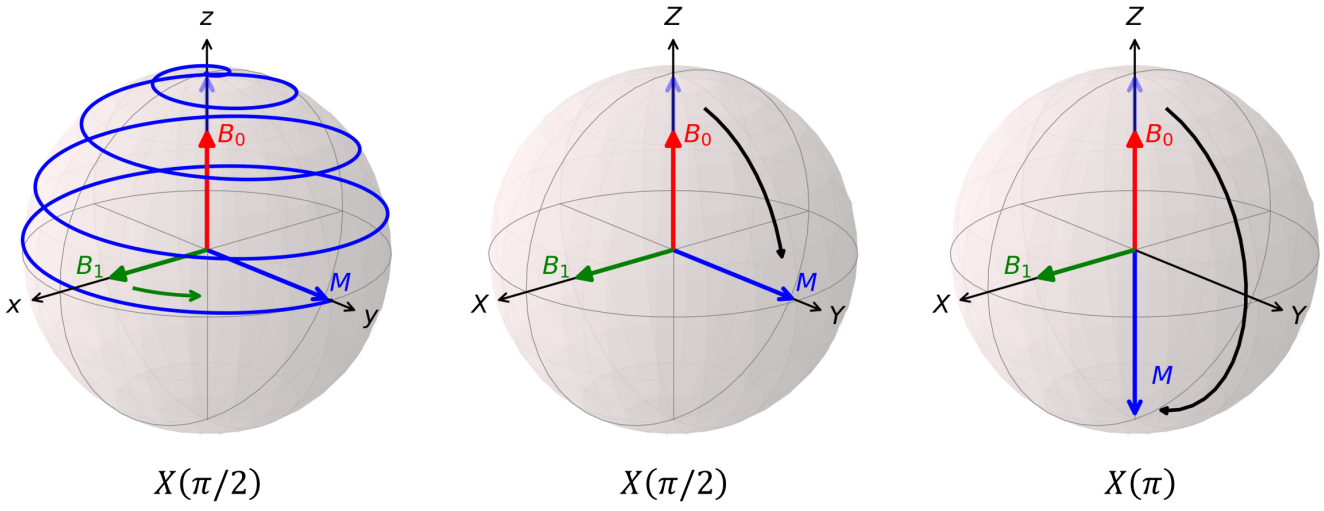

Figure 1: The basic process of NMR. On the first image, we demonstratre how would the M magnetization develop overtime due to the B_1 and B_0 magnetic fields in the lab system. It precesses while rotating away from its equilibrium state. The other two images are in the rotating frame, showing a rotation of 90° and 180° along the X-axis using a pulsed B_1 magnetic field in the X direction.

2.1 The amplitude of NMR signal

We have seen that the magnetization of the material can be tilted out of its equilibrium position if we apply irradiation with a frequency matching the Larmor frequency. After this, we measure the signal of the sample, which is induced in the coil as the magnetization rotates at the Larmor frequency. But how large is this measured voltage? Suppose the magnetization of the sample completely fills the receiver coil with N turns. A voltage is induced in the coil because the changing magnetic field of the sample results in a changing flux along the surface of the coil. Thus, the induced voltage is:

$$U = \mu_0 M A N \omega_\mathrm{L},$$

where μ_0 is the vacuum permeability, M is the magnetization of the sample, A is the cross-sectional area of the receiver coil, N is the number of turns of the coil, and ω_L is the Larmor angular frequency. The magnetization generated in the sample can be obtained by considering a two-state system which is in thermal contact with a heat reservoir at temperature T. We place this system in a homogeneous magnetic field of magnitude B. The number of states can be derived from Boltzmann statistics, and thus the magnetization is:

$$M = \frac{\rho_0 \gamma^2 \hbar^2 I(I+1)}{3 k_\mathrm{B} T} B,$$

where $\rho_0 = \frac{N_\mathrm{spin}}{V_\mathrm{sample}} = \frac{1}{V_\mathrm{cell}}$ is the spin density, I is the nuclear spin (1/2 in the case of a proton), k_B is the Boltzmann constant, and T is the absolute temperature. From here, we can get the Curie susceptibility of the nuclei:

$$\chi_\mathrm{Curie} = \frac{\mu_0 \gamma^2 \hbar^2 I(I+1)}{3 k_\mathrm{B} T \cdot V_\mathrm{cell}}.$$

This is a very small susceptibility. Let's take a specific example! How much magnetic moment of iron corresponds to the magnetic moment of 100 μl of water when placed in a $B = 7$ T magnetic field? First, let's calculate the spin density. This means determining how many hydrogen nuclei are present in a unit volume. The density of water is known ($\rho_v = 1000\ \frac{\mathrm{kg}}{\mathrm{m}^3}$) and its molar mass ($M_v = 18\ \frac{\mathrm{g}}{\mathrm{mol}}$), and we also know that each water molecule contains two hydrogen atoms. Thus, the spin density is:

$$\rho_0 = \frac{2N}{V} = \frac{2N_\mathrm{A} \cdot \frac{m}{M_v}}{V} = \frac{2N_\mathrm{A} \cdot \rho_v}{M_v} = \frac{2 \cdot 6 \cdot 10^{23}\ \frac{1}{\mathrm{mol}} \cdot 1000\ \frac{\mathrm{kg}}{\mathrm{m}^3}}{0{,}018\ \frac{\mathrm{kg}}{\mathrm{mol}}} = 6{,}7 \cdot 10^{28}\ \frac{1}{\mathrm{m}^3}.$$

Let's assume a temperature of 300 K, thus the magnetization is:

$$M = \frac{6{,}67 \cdot 10^{28}\ \frac{1}{\mathrm{m}^3} \cdot \left(2\pi \cdot 42{,}58\ \frac{\mathrm{MHz}}{\mathrm{T}}\right)^2 \cdot \left(1{,}05 \cdot 10^{-34}\ \mathrm{Js}\right)^2 \cdot \frac{1}{2} \cdot \left(\frac{1}{2}+1\right)}{3 \cdot 1{,}38 \cdot 10^{-23}\ \frac{\mathrm{J}}{\mathrm{K}} \cdot 300\ \mathrm{K}} \cdot 7\ \mathrm{T} = 0{,}022\ \frac{\mathrm{A}}{\mathrm{m}}.$$

The magnetic moment of 100 μl of water is $\mu_v = M \cdot V = 0.022\ \frac{\text{A}}{\text{m}} \cdot 10^{-7}\ \text{m}^3 = 2.2 \cdot 10^{-9}\ \text{Am}^2$. How many iron magnetic moments does this correspond to? Iron is ferromagnetic, meaning it has saturated moments, so the magnitude of the moments is $g\mu_\text{B}$ per unit cell. The required number of iron atoms is therefore

$$N_\text{Fe} = \frac{\mu_v}{g\mu_\text{B}} = \frac{2{,}2 \cdot 10^{-9}\ \text{Am}^2}{1{,}855 \cdot 10^{-23}\ \text{Am}^2} = 1{,}186 \cdot 10^{14}$$

The required mass of iron is the following:

$$m_\text{Fe} = M_\text{Fe} \cdot \frac{N_\text{Fe}}{N_\text{A}} = 55{,}85\ \frac{\text{g}}{\text{mol}} \cdot \frac{1{,}186 \cdot 10^{14}}{6 \cdot 10^{23}} = 11\ \text{ng}\ .$$

Thus, the magnetization of 100 mg of water corresponds to the magnetization of only 11 ng of iron, representing a 7-order of magnitude difference! This illustrates how small the magnetization we measure is. Let's return to the question of the induced voltage in the coil. Consider a coil with $N = 10$ turns and a cross-sectional area with a diameter of 5 mm, and a Larmor frequency of 300 MHz. The induced voltage is:

$$U = \mu_0 MAN\omega_\text{L} = 4\pi \cdot 10^{-7}\ \frac{\text{Vs}}{\text{Am}} \cdot 0{,}022\ \frac{\text{A}}{\text{m}} \cdot (2{,}5 \cdot 10^{-3}\ \text{m})^2 \pi \cdot 10 \cdot 2\pi \cdot 300 \cdot 10^6 \frac{1}{\text{s}} = 10\ \text{mV}\ .$$

From the above considerations, it is apparent that the magnitude of the NMR signal increases with the square of the Larmor frequency, that is, with the square of the applied magnetic field. One factor arises from the Boltzmann population difference, and the other from the Faraday induction factor. More precise considerations (taking into account bandwidth) yield a factor of $\frac{9}{4}$.

2.2 FID

In the Free Induction Decay (FID) acquisition, a single 90° pulse is applied, causing the spins to align perpendicular to B_0, so that the X-Y component reaches its maximum value, and then decays exponentially due to the T_2 relaxation process occurring in the X-Y plane. There are two notable points regarding this. Firstly, the decay of the amplitude of the voltage will only be exponential if the frequency of the irradiating B_1 field exactly matches the Larmor frequency. Generally, an oscillatory signal is observed with an exponential envelope. Secondly, the time constant of this process is not actually T_2 as stated in the Bloch equations, because what is truly measured is the sum of many moments with due consideration to their phase, and since the B_0 magnetic field is never perfectly homogeneous in reality, the spins will precess at slightly different Larmor frequencies, leading to rapid dephasing. Although the spins are not relaxed in the x-y direction, the signal decreases because the components with different phases cancel each other out. This relaxation due to field inhomogeneity is characterized by the so-called T_2^* relaxation time (which we may also refer to as the reversible relaxation time, in contrast to the T_2 relaxation time, sometimes called the irreversible relaxation time). In practice, when using any pulse type, we wait $10 \cdot T_1$ time between pulses (or pulse sequences) to allow sufficient time for the magnetization to return to the Z direction. Sometimes, we intentionally do not wait this long, for example, when acquiring T_1 contrast images in MRI measurements.

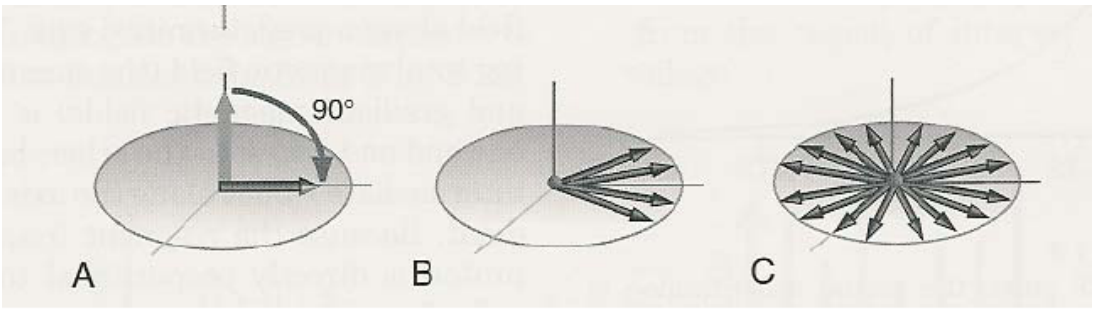

Figure 2: The scheme for FID. After the initial $\pi/2$ pulse, the frequency of the detected signal is $(\omega_\text{L} - \omega)/2\pi$ (where $\omega/2\pi$ is the frequency of the irradiating field), and the decay is exponential because the coherence of the nuclear spins is lost in the X-Y plane.

2.3 FT-NMR

In NMR techniques, the measured signal is detected as a function of time. It automatically follows that the Fourier transform (FT) of the detected signal gives the frequency spectrum of the NMR signal. Before proceeding further, we need to become familiar with an important concept, the so-called complex (or two-channel) Fourier transform.

The definition of the FT operation is:

$$\hat{x}(\omega) = \frac{1}{\sqrt{2\pi}} \int_{-\infty}^{\infty} x(t) \cdot \mathrm{e}^{-\mathrm{i}\omega t} \, \mathrm{d}t$$

(where $\hat{x}(\omega)$ is the Fourier transform). From this, it is evident that after the FT, we obtain two independent functions (real and imaginary parts), which are defined for both positive and negative frequencies. Later, we will see that in NMR techniques, the measured signal can have negative frequencies as well, or more precisely, it is important that the frequency is measured with the correct sign. However, if $x(t)$ is a real function, then the values of the real part of the Fourier transform at negative and positive frequencies are the same. Similarly, the values of the imaginary part of the FT are the same in absolute value at frequencies with opposite signs but equal magnitude, i.e., $\hat{x}(-\omega) = \hat{x}(\omega)^*$, where $*$ denotes the complex conjugate. This shows that if we only have a single real data set $x(t)$, the sign of the oscillatory signal's frequency cannot be determined[3].

The solution to this is provided by the so-called two-channel FT: the measured NMR signal is not just a single time-dependent data series but also contains another data series shifted by 90 degrees at a given $\omega_{\mathrm{LO}}/2\pi$ working frequency. This can also be understood as measuring two components of a vector in a perpendicular coordinate system. These two time-dependent data series are considered as the real and imaginary parts of $x(t)$, respectively, and after performing the FT operation, the frequency is uniquely determined.

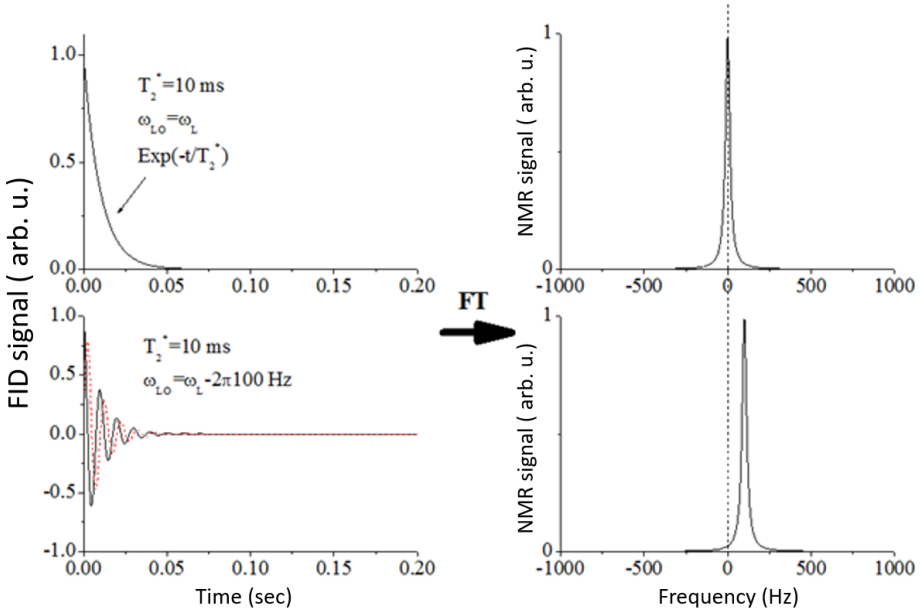

Figure 3: Fourier transforms of different FID signals. The FT of the two FIDs on the left are shown on the right. The black solid and red dashed lines represent the detected signals that are shifted by 90 degrees relative to each other.

Figure 3. shows two examples. If the FID is such that in one channel we observe an exponential decay and in the other channel an identical 0 signal, its FT is a Lorentzian function[4], centered at zero frequency. This signal shape occurs when the NMR spectrometer's operating frequency ($\omega_{\mathrm{LO}}/2\pi$) exactly matches the Larmor frequency of the nuclear spins ($\omega_{\mathrm{L}}/2\pi$). Otherwise, we find an oscillation with an exponential envelope in the FID, as shown in the other figure. The signals in the two channels (continuous black and dashed red lines) are exactly 90 degrees out of phase with each other. The oscillation frequency is the difference between the NMR operating frequency and the Larmor frequency, $(\omega_{\mathrm{L}} - \omega_{\mathrm{LO}})/2\pi$. The FT of this signal shape is also Lorentzian, with the center at the frequency $(\omega_{\mathrm{L}} - \omega_{\mathrm{LO}})/2\pi$. It is evident that the zero of the Fourier transformed spectra always corresponds to the Larmor frequency of the nuclei. In practice, the Larmor frequency of a given standard compound is usually considered as zero, and the shifts relative to this are measured in ppm[5] units.

We note that the real NMR signal shape is rarely Lorentzian, as it is primarily determined by the inhomogeneity

[3]This is analogous to examining the projection of a point onto the x or y axis that moves on the unit circle, where the direction of motion cannot be determined.

[4]The Lorentzian function is particularly significant because exponential decays are common in physical processes, and in such cases, the frequency spectrum has a Lorentzian shape. Another common case is when the decay follows a Gaussian function, its FT is also a Gaussian function.

[5]The shift is measured in Hz and divided by the Larmor frequency measured in MHz.

of the magnetic field, which can result in an arbitrary shape. Consequently, the time-dependent signal shape is also most often not exponential.

Due to the FT technique, it is worth mentioning how the fundamental parameters of the NMR spectrum depend on the parameters of real-time digitization. The operation of the receiver unit of an NMR spectrometer is very similar to that of an oscilloscope: it measures data points at a given sampling frequency, f_0, over N points (i.e. every $1/f_0$ seconds). Accordingly, the resulting FT spectrum ranges from $-f_0/2$ to $f_0/2$. The spectral resolution of the spectrum is f_0/N.

2.4 The Spin-echo

To counteract the decoherence caused by the T_2^* relaxation mentioned in the FID, as well as the so-called dead-time that occurs in the equipment, the spin-echo pulse sequence was developed. This consists of a 90° pulse followed by a 180° pulse applied after a delay of τ. The spins, after they were rotated by 90°, experience a certain amount of decoherence while waiting τ time, since those nuclei in regions where the local magnetic field is slightly stronger will precess faster. Afterwards, a 180° pulse reverses the direction of the spins, which acts as if the flow of time has been reversed: the fastest precessing spins are now at the back. The individual spins continue to precess at the same angular frequency as during the decoherence period, but now the process proceeds in the opposite direction from the perspective of coherence. By symmetry, it is evident that after a time τ following the 180° pulse, the spins are once again aligned, and the signal known as the spin-echo appears. A visual demonstration can be found here: Wikipedia/Spin_echo.

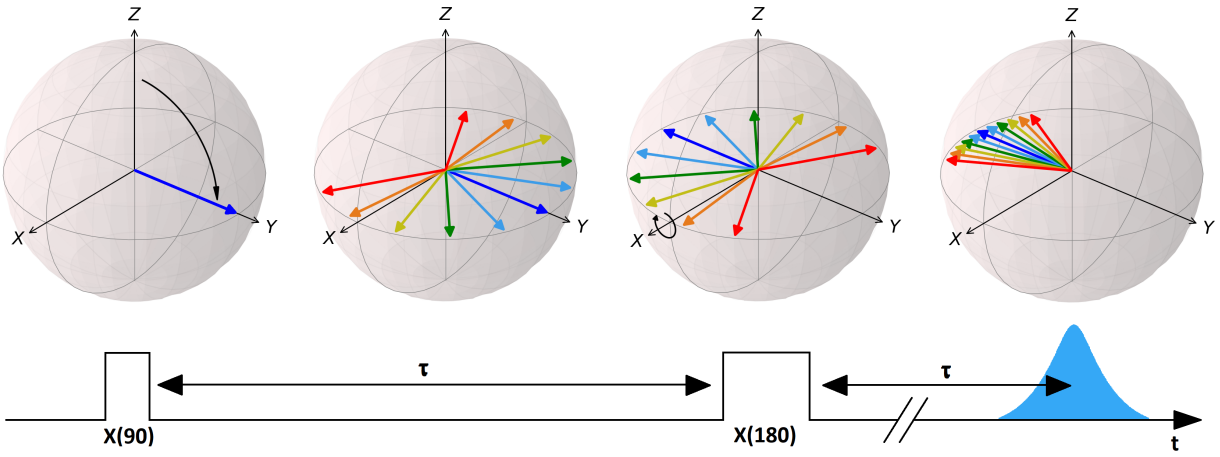

Figure 4: The scheme of the spin-echo. After the $\pi/2$ pulse in the X direction, we observe an FID in the Y direction, which decays with the T_2^* relaxation time. This is followed by a π pulse after a time interval τ, which reverses the direction of time for the spins. Consequently, after another τ time, we observe a spin-echo in the $-Y$ direction.

In MRI techniques, we also encounter the so-called gradient echo. The essence of this method is that a magnetic field gradient is created inside the magnet (the magnitude of the z-direction magnetic field becomes position-dependent). As a result, the Larmor frequency of the nuclei becomes position-dependent, which leads to a faster decoherence and an apparently shorter T_2^*. After a short time, by reversing the sign of the gradient, we obtain a spin echo, in a manner entirely analogous to the usual spin-echo.

2.5 The CP pulse sequence

The essence of the Carr-Purcell[6] (CP) pulse sequence is that it enables the measurement of the true T_2 relaxation time. We have seen that the relaxation time of the envelope of the FID or the spin-echo is T_2^*, the so-called reversible decoherence time. The origin of this term is that the decoherence caused by magnetic field inhomogeneities in the sample – as shown by the spin-echo technique – is reversible, and the coherence can be restored. The true T_2, also known as the irreversible decoherence or spin-spin relaxation time, gets its name from physical processes that, according to the second law of thermodynamics, result in a true loss of information, leading to decoherence. The process causing T_2 involves the indistinguishability among the nuclear spins interacting with each other (typically through magnetic dipole-dipole interactions). The CP pulse sequence consists of applying further π pulses after the first spin-echo, which results in alternating spin-echoes in the Y and $-Y$ directions. The envelope of the magnitudes of these spin-echoes corresponds to the T_2 relaxation time.

[6]H. Y. Carr and E. M. Purcell: "Effects of Diffusion on Free Precession in Nuclear Magnetic Resonance Experiments," Phys. Rev. **94**, 630 (1954).

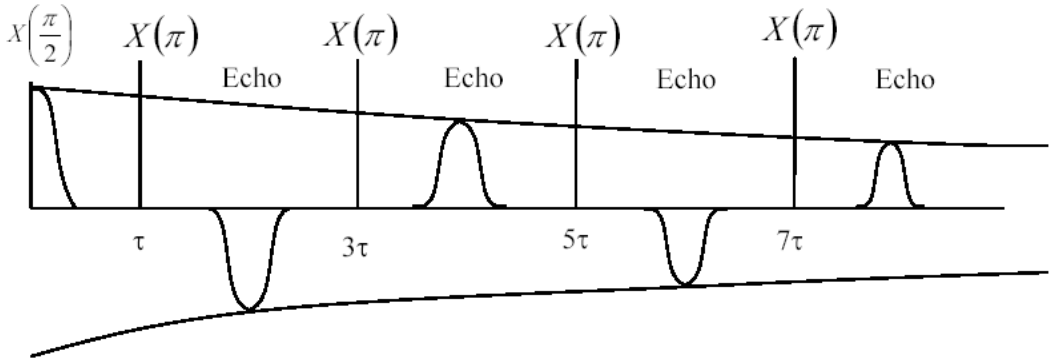

Figure 5: The scheme of the CP pulse sequence. The X-axis π pulse, which generates the first spin-echo, is followed by further pulses along the X direction, resulting in alternating spin-echoes along the Y and $-Y$ directions. Their magnitudes decay following the T_2 relaxation time.

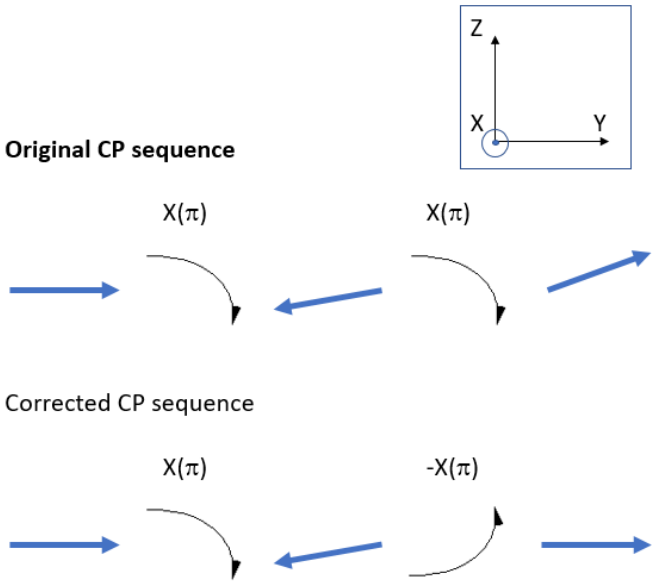

Figure 6: The magnetization in the X-Y plane as viewed from the X direction, when the spin-echo is just formed (i.e., the magnetization is aligned along the Y direction). In cases where the π pulse duration is not perfect, phase errors accumulate in the original CP pulse sequence, whereas in the corrected scheme, these errors are compensated. The coordinate system is shown in the upper right corner.

The phase error in the CP sequence can be corrected by applying alternating $X(\pi)$ and $-X(\pi)$ pulses. However, historically, in the 1970s, it was difficult to implement this, which led to the introduction of the following sequence. This sequence has automatic phase correction, even though all pulses are given in the same direction.

2.6 The CPMG pulse sequence

The disadvantage of the CP pulse sequence is that if the set π pulse length is not exactly 180°, phase errors will accumulate, which will distort the measurement. This issue is resolved by the CPMG[7] (Carr-Purcell-Meiboom-Gill) pulse sequence, which works the following way: after the first X-axis $\pi/2$ pulse, the echoes are created with Y-axis π pulses, thus the spin-echoes form along the Y axis.

Although we saw earlier that the CP pulse sequence can also be corrected by alternating the phase direction of the rotation, it turns out that the CPMG sequence has automatic error correction, even when using pulses in the same direction.

[7]S. Meiboom and D. Gill: "Modified Spin-Echo Method for Measuring Nuclear Relaxation Times," Rev. Sci. Instrum. **29**, 688 (1958).

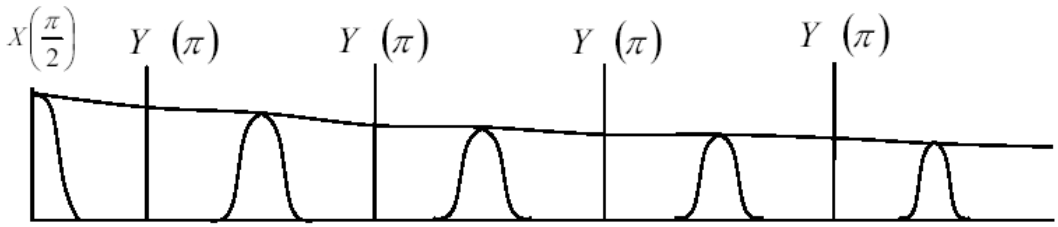

Figure 7: The scheme of the CPMG pulse sequence. The starting 90° rotation around the X axis is then followed by a 180° rotation around the Y axis at intervals of 2τ. The spin echoes align in the same direction, and their envelope decays with the T_2 relaxation time.

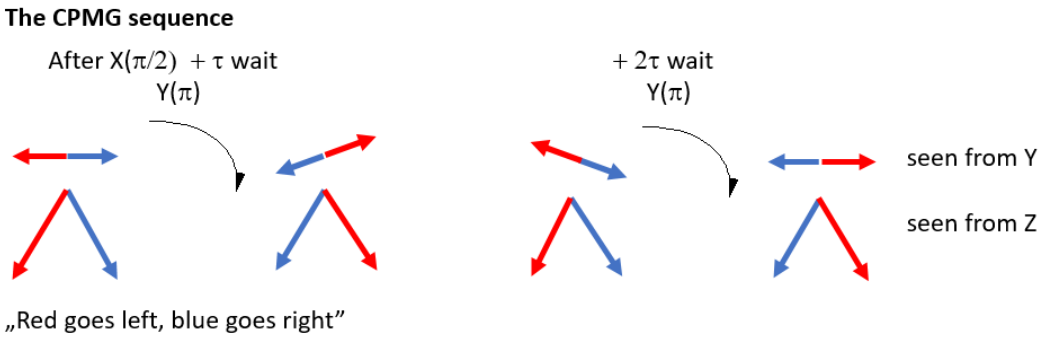

Figure 8: The scheme of the spin evolution in time using the CPMG pulse sequence. Top row: viewed from the Y direction, bottom row: viewed from the Z direction. For simplicity, we assumed that initially the individual magnetization directions are exactly in the XY plane after the first $X(\pi/2)$ pulse. According to the figure, the magnetization direction marked in red always moves to the left, while the direction marked in blue always moves to the right, depending on where they are located relative to the average Larmor frequency.

This automatic error correction is demonstrated in Figure 8. Historically, at the time of the creation of the original CP and CPMG sequences, it was not technically possible to freely adjust the phase, which made the automatic error correction of the CPMG sequence a clear advantage over the CP sequence.

2.7 Inversion recovery

Az *inversion recovery* szekvencia a T_1 relaxációs idő mérésére szolgál. Ebben az esetben az előzőekkel ellentétben az első gerjesztő pulzus 180°-os, míg a kiolvasó pulzus 90°-os. A 90°-os pulzus után mért FID kezdő amplitúdója az ábrán látható módon változik a gerjesztő és a kiolvasó pulzus időbeli távolságának függvényében. Ha például azonnal alkalmaznánk a kiolvasó pulzust, akkor az összesen 270°-os elforgatásnak felelne meg és egy negatív FID-t kapnánk. Ehhez képest t idő elteltével a spinek z irányba relaxálnak, így az FID abszolút értéke egyre kisebb lesz. Amikor a relaxáció éppen a felénél tart, akkor nem kapunk jelet és ezután pozitív irányú spint fogunk leforgatni, amiből pozitív FID-t kapunk. Végtelen idő múlva a spinek visszaállnak az eredeti irányba és ismét maximális amplitúdójú, de ezúttal pozitív FID-t kapunk (a standard FID-t). A módszer kombinálható a hagyományos spin-echo-val, azaz a második, $\pi/2$-es pulzus helyett egy $\pi/2$- π pulzus-sorozatot is használhatunk. Az inversion-recovery módszernél fontos, hogy la. $10 \cdot T_1$ ideig várjunk két sorozat között.

The *inversion recovery* sequence is used for measuring the T_1 relaxation time. Unlike the previous methods, in this case, the first excitation pulse is 180°, while the readout pulse is 90° long. The initial amplitude of the FID measured after the 90° pulse varies with the temporal separation between the excitation and readout pulses, as shown in the figure. For instance, if the readout pulse were applied immediately, it would correspond to a total rotation of 270°, resulting in a negative FID. Over time the spins relax towards the Z direction, reducing the absolute value of the FID. When the relaxation is halfway, no signal is observed, and after that, the spins rotate in a positive direction, producing a positive FID. After an infinite amount of time, the spins return to their original direction, and a maximum amplitude, positive FID (the standard FID) is obtained. The method can be combined with the conventional spin-echo, meaning that instead of a second $\pi/2$ pulse, a $\pi/2$ - π pulse sequence can also be used. In the inversion-recovery method, it is important to wait approximately $10 \cdot T_1$ between sequences.

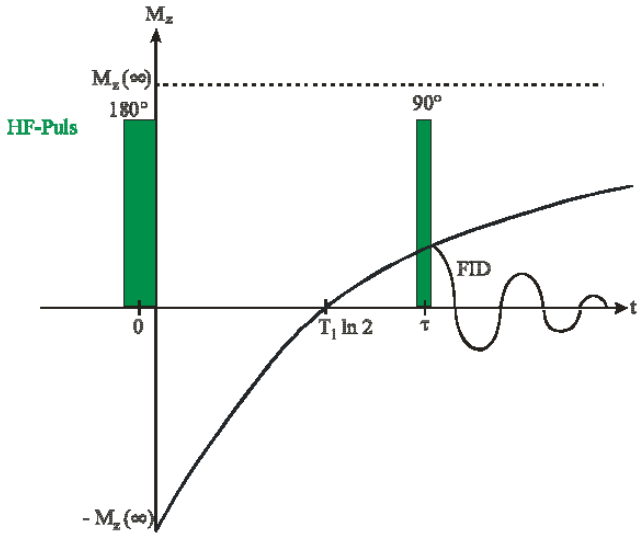

Figure 9: The diagram of the inversion recovery pulse sequence. After an initial π pulse, the state of the spins is read out with a subsequent $\pi/2$ pulse.

2.8 Phase cycling

The method used to eliminate imperfections in the circuits of an NMR device (such as dead time, ringing, offset problems, amplifier and quadrature asymmetry, etc.) is known as phase cycling. In a simple example, consider that the digitizing circuit for the NMR signal has a voltage offset component after the pulses are acquired. This component distorts the resulting signal in the FT spectrum, potentially leading to false FT components, and so on. However, this signal can be eliminated in the case of an FID by taking two FIDs: with the first $\pi/2$ pulse in the X direction and the second in the $-X$ direction, then subtracting the two FIDs from each other. In the language of Tecmag equipment, this is written as follows:

$\Phi_1 =$ 0 2
$\Phi_{\mathrm{Acq}} =$ 0 2

Here, Φ_1 denotes the phase of the first pulse, and Φ_{Acq} refers to the phase of the receiver during the acquisition. The values 0, 1, 2, 3 correspond to the pulses along the X, Y, $-X$, and $-Y$ directions respectively. In this method, two FIDs are acquired, and naturally, this measurement must be performed with an even number of samplings.

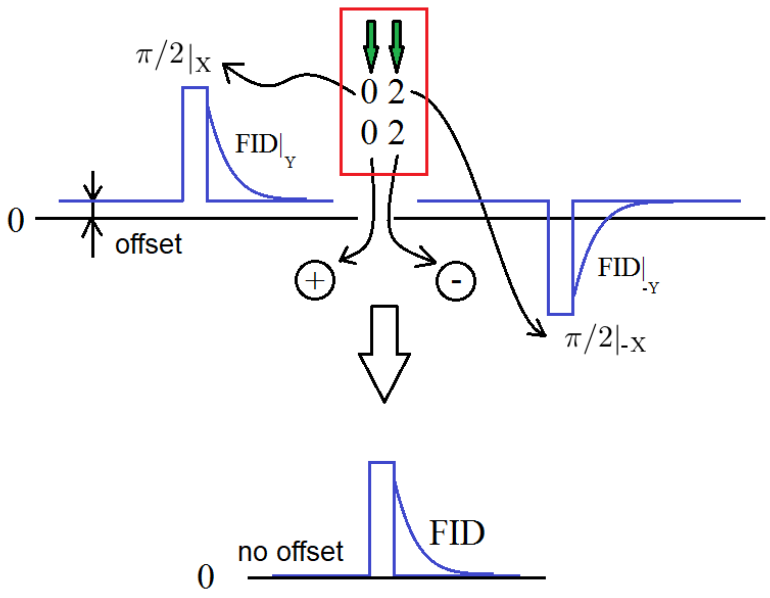

Figure 10: Using phase cycling to subtract offset in FIDs.

In another example, we would like to subtract the FID after the first pulse in a spin-echo measurement. The syntax is the following:

$\Phi_1 =$ 0 2
$\Phi_2 =$ 0 1
$\Phi_{\mathrm{Acq}} =$ 0 0

Here, Φ_2 denotes the direction of the π pulse. The drawback of this method is that although the FID is subtracted, the π pulse itself is measured by the equipment, which could cause issues with the recorded data.

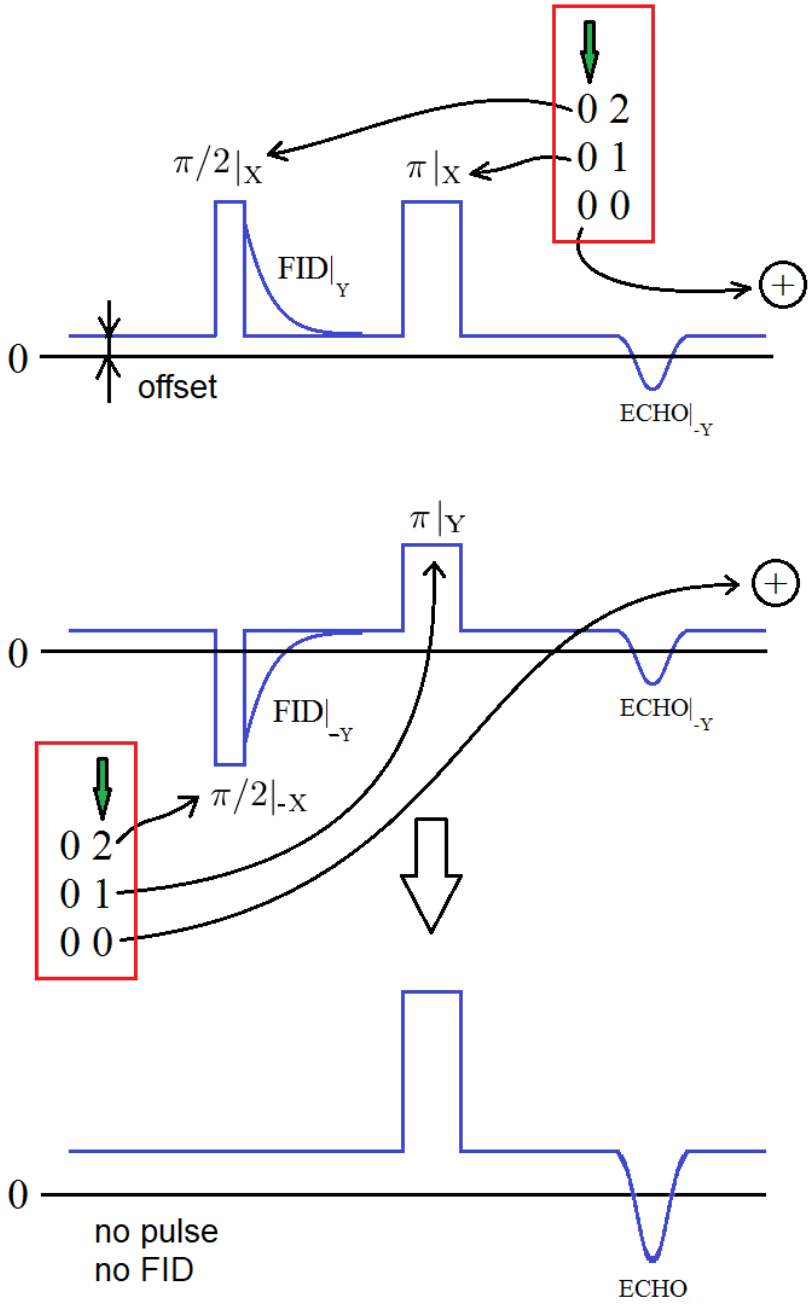

Figure 11: Phase cycling for spin echo

An improved version of this method uses 4 pulses, allowing both the FID and the second pulse to be subtracted, leaving the final result to contain only the spin echo:

$\Phi_1 =$ 0 0 0 0
$\Phi_2 =$ 0 2 1 3
$\Phi_{\mathrm{Acq}} =$ 0 0 2 2

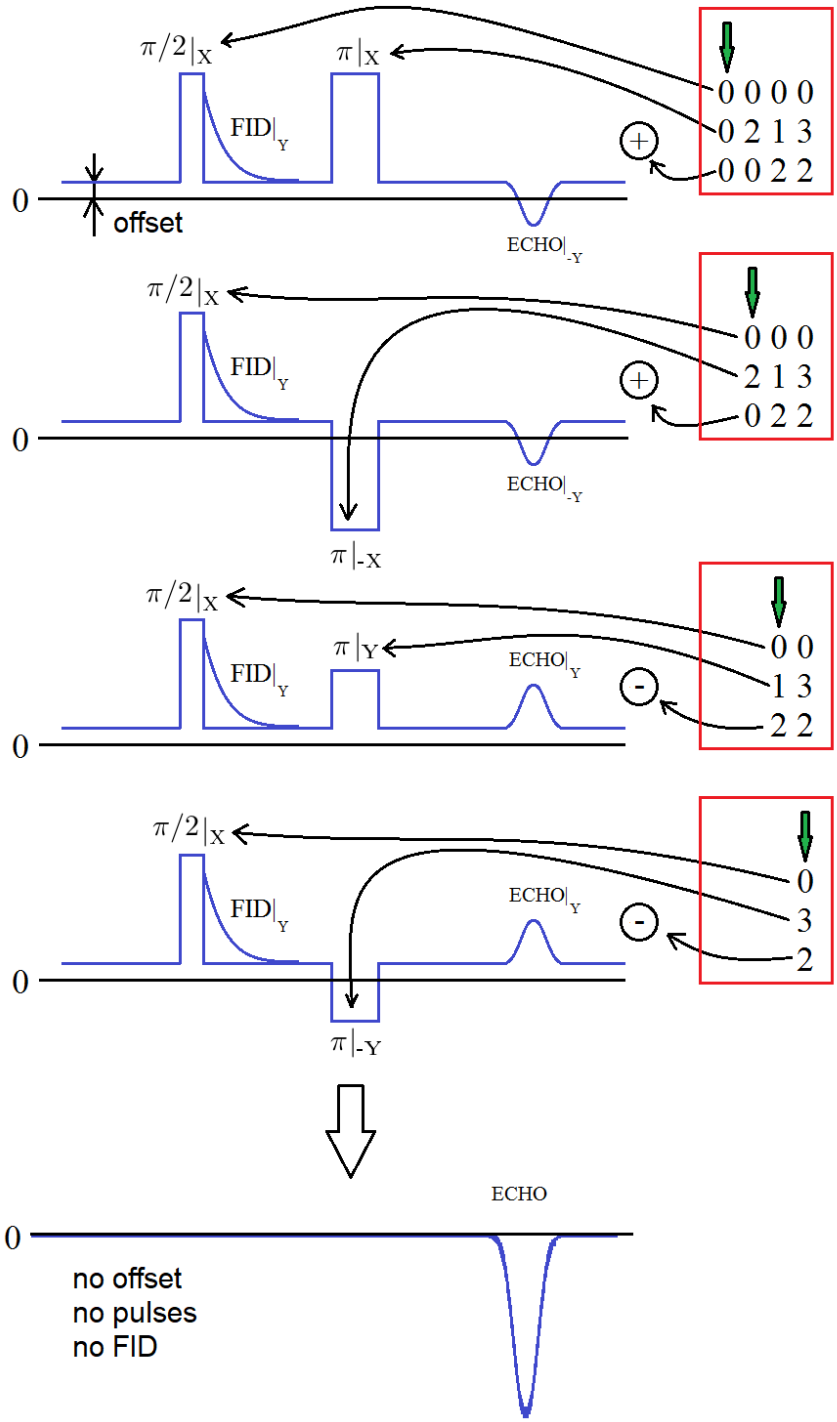

Figure 12: A modified version of phase cycling for spin echo

It can be seen that it is advantageous to measure a complete series by cyclically permuting the phases (hence the origin of the term *phase cycle*), which for the last example looks as follows:

$$\Phi_1 = \; 0\,0\,0\,0\,1\,1\,1\,1\,2\,2\,2\,2\,3\,3\,3\,3$$
$$\Phi_2 = \; 0\,2\,1\,3\,1\,3\,2\,0\,2\,0\,3\,1\,3\,1\,0\,2$$
$$\Phi_{31} = \; 0\,0\,2\,2\,1\,1\,3\,3\,2\,2\,0\,0\,3\,3\,1\,1$$

Finally, returning to the CP and CPMG sequences, it can be understood that phase cycling can be performed most simply by alternating the phase of the π pulse sequences with phases 0 and 2 for CP, and with phases 1 and 3 for CPMG. This means that for a given pulse train, we do not modify it, but instead take successive series with a phase

increment of 2. The specific implementation will be discussed later at the end of the description, but in practice, this means that for the corrected CP, we apply a so-called 1/2D cycle with phases 0 and 2, and a 1D cycle also with phases 0 and 2, while for CPMG, no 1/2D cycle is required, only a 1D cycle with phases 1 and 3. By using a 1/2D cycle with phases 1 and 3 for CPMG, it behaves like the original CP pulse sequence, which does not correct errors.

3 The experimental setup

3.1 The basis of heterodyne detection

A fundamental component of modern telecommunications and NMR spectroscopy is the so-called heterodyne technique (Wikipedia/Superheterodyne_receiver). The essence of this method is that the frequency of the detected signals remains constant in the transmitter-receiver, independent of the carrier wave frequency. Imagine building a radio transmitter-receiver that operates broadband, in the $10-300$ MHz range. This is a difficult task, because such a wide frequency range cannot be covered by a single high-quality device, and for every narrower frequency band (e.g., in 10 MHz intervals), separate devices (such as amplifiers, demodulators, etc.) would be needed. In a heterodyne receiver, this challenge is addressed by encoding the information into a signal with a given frequency within a narrow range called the *intermediate frequency* (IF). This signal is mixed with the signal of a broadband-tunable *local oscillator* (LO) using a nonlinear electronic component (most commonly a Schottky diode) known as a mixer. Reminder: from the trigonometric addition formulas, it can be understood that in this case, the mixer output produces the frequencies RF = LO+IF and RF = LO−IF (called *radiofrequency*, RF), which are transmitted by the transmitter. In the receiver, tuning into the appropriate frequency band involves selecting the correct LO frequency, with which the receiver mixes the incoming RF signal, producing the IF signal again (frequencies such as $2\mathrm{LO}+\mathrm{IF}$ also appear, but these can be filtered out), which then can be detected. The NMR spectrometer is essentially a highly sensitive transmitter-receiver (more accurately compared to a radar): it emits a high-energy pulse and then detects the low-energy response from the sample.

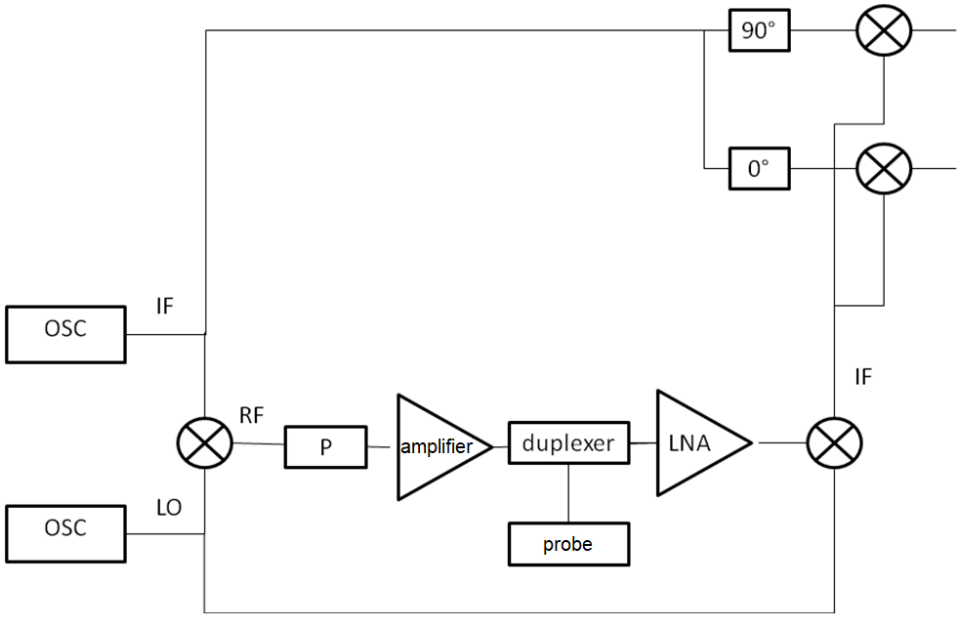

Figure 13: The block diagram of an NMR device operating on the heterodyne principle. P: pulse generator, modulates the RF signal with pulses; amplifier: power amplifier, typically 100 W; LNA: low noise amplifier, the remaining components are described in the text.

Speaking of the operation of the device, it is important to further detail the question of phase: the clock signal of the local oscillator can be considered as the signal with 0 phase, relative to which the emitted signal has a given phase, and this is also the reference for measuring the detected signal. Accordingly, a rotation around the X axis (the axis names were defined above) corresponds to no phase shift relative to the clock signal, the Y axis corresponds to a 90° shift, $-X$ corresponds to a 180° shift, and so on.

3.2 Quadrature detection

As mentioned above, the NMR signal is nothing more than a low-amplitude radio frequency voltage pulse, whose phase is shifted relative to the local oscillator[8]. Thinking of the NMR signal as a complex vector, it is apparent that we can only fully reconstruct the NMR signal if we measure both the amplitude of the components that are in phase and 90° out of phase relative to the local oscillator. The simultaneous measurement of these two signals is called quadrature detection, and this is technically achieved by the 90° phase shifter shown in the NMR block diagram. From the signals measured in quadrature in the two channels (CH_x and CH_y), any signal with phase Φ can be mixed using the combination $CH_x \cdot \cos\Phi + CH_y \cdot \sin\Phi$. The signals in the two channels are not independent of each other: they are connected by the Kramers-Kronig transformation. In this sense, the measured NMR signal is redundant, but for technical reasons, it is still beneficial to measure both. The figure symbolically shows the 90° phase shifter, also known as a 90° hybrid RF circuit.

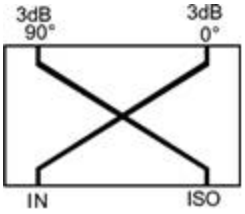

Figure 14: The schematic of the 90° hybrid circuit. At the output of the circuit, half of the power of the IN and ISO input signals is superimposed, with one component's phase shifted by 90°.

3.3 The phase of the pulses

In the above, we have demonstrated how to generate pulses that rotate the magnetization along the X, Y, $-X$, and $-Y$ directions in the rotating reference frame. It is reasonable to ask: 1) how these pulses can be physically generated, 2) what exactly this phase means, and 3) what the frequency of the rotating reference frame means in a realistic case, where the nuclear spins do not rotate at the same frequency.

The answer to question 3) is that it is practical to consider the frequency of the rotating reference frame as the *average* Larmor frequency of the nuclear spins. As we have seen in the context of T_2^*, the cause of the reversible decoherence of the nuclear spins (and thus of the spin-echo) is the distribution of Larmor frequencies. The most common cause of this distribution is the inhomogeneity of the magnetic field, either due to the external field of the magnet or due to impurities in the sample.

To understand the phase of the pulses, let us consider the nature of detection: the pulses are generated by the clock signal of the NMR device, but at the same time, this clock signal is also used for the mixing, which gives us the detected signal. Our statement is that the X coordinate direction is completely arbitrary; we speak of a pulse rotating around the X direction when the voltage on the coil is generated without phase shift relative to the LO phase. Similarly, to generate pulses rotating around the Y, $-X$, and $-Y$ directions, we shift the emitted signal by 90°, 180°, and 270°, respectively, relative to the LO signal. (We note that it would be difficult to create a broadband frequency shifter, so all this is done in the fixed frequency IF signal used to mix for the RF signal.)

To understand the effect of the pulses emitted at different phases, consider that the magnetic field created in the solenoid is linearly polarized, which can be decomposed into two circularly polarized components rotating in opposite directions. Due to the external DC magnetic field, the direction of the Larmor precession is well-defined, and only one of the components will rotate in the same direction as the precession. It is easy to see that when we shift the phase of the current generating the linearly polarized magnetic field, for instance by 90°, it acts as if we rotated the circularly polarized magnetic field by 90° in the direction of its rotation. From this, it becomes evident that the phase shifts mentioned above indeed cause the magnetic fields generating magnetic resonance to rotate. This corresponds precisely to the effect of generating magnetic fields rotating along different directions in the rotating coordinate system.

3.4 Duplexer

The role of the duplexer is to send voltage pulses of several 100 V from the power amplifier to the sample during irradiation, and then direct the sample's induced response in the coil of a few μV to the low-noise preamplifier. This can be achieved using the duplexer shown in the following figure, which uses two pairs of diodes and a so-called $\lambda/4$ cable[9].

[8] There are numerous causes for phase shifts: the phase shift of the entire RF circuit, finite signal propagation speeds in the cables, and every RF device has a finite phase shift.

[9] λ is the wavelength of the RF radiation in the cable.

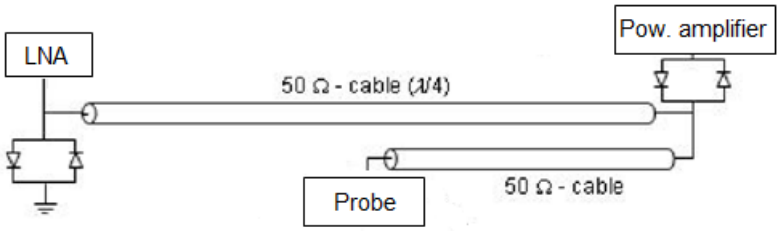

Figure 15: The duplexer

The essence of the arrangement is that the diode pair after the power amplifier opens while irradiation of the sample. At the same time, the other diode pair is open to the ground, so the LNA is also grounded and thus protected from high-energy pulses. The $\lambda/4$ cable functions analogously to an open-ended pipe with a length of $\lambda/4$: the wave's amplitude is maximal at the open end, while it is zero at the closed end. In our case, the LNA corresponds to the closed end, while the RF amplitude is maximal at the probe. Both diode pairs close when detecting the weak NMR signal from the nuclei, allowing the signal to fully reach the LNA.

3.5 Probehead

Both during the transmission of the RF pulse and the reception of the detected NMR signal, it is crucial that the signals are effectively transmitted from the equipment to the probe and vice versa. From the theory of high-frequency networks, it is known that energy propagates efficiently (without reflections) in a transmission line of a given characteristic impedance if it is terminated with a real impedance equal to this characteristic impedance. The most commonly used BNC cable has a characteristic impedance of 50 Ω, so the probehead must also present a real impedance of this value. It is clear that it is not favourable to create this impedance with a resistive element or a single inductor, but rather with an RF resonant circuit, as shown in the following figure. By adjusting the capacitances of the capacitors, we can ensure that this circuit presents a real 50 Ω impedance. Simply put, the operation of the circuit is done via adjusting the tuning capacitor C_T to set the frequency at which we want to measure, and using the matching capacitor C_M to minimize reflections. In reality, the two parameters are not independent of each other.

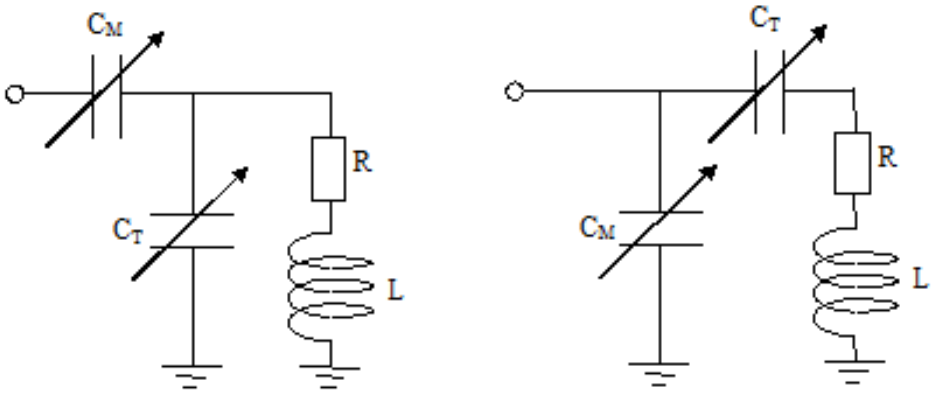

Figure 16: The structure of the resonant circuits used in NMR measurement. C_T is the so-called tuning capacitor and C_M is the matching trimmer capacitor. The circuit on the left is used below 100 MHz, while the circuit on the right is used for frequencies above that.

The figure shows two circuits that are transformable into each other and are therefore ideally equivalent. However, due to the presence of so-called stray capacitances, they are not truly equivalent, and experience shows that the circuit on the left is better below approximately 100 MHz, while the circuit on the right performs better above approximately

100 MHz. Stray capacitances arise when electrodes at ground potential and those not at ground potential are close to each other. For instance, the ends of the coil are not at the same potential because there is a high voltage drop across the coil, so a stray capacitance also appears there.

3.6 Matching the probehead 50 Ω

The task in the above-described RF circuit is to select the values of C_{T} and C_{M} so that the resulting impedance of the circuit is 50 Ω at the Larmor frequency. This can be accomplished using a so-called magic-T, a *180°-RF hybrid* circuit.

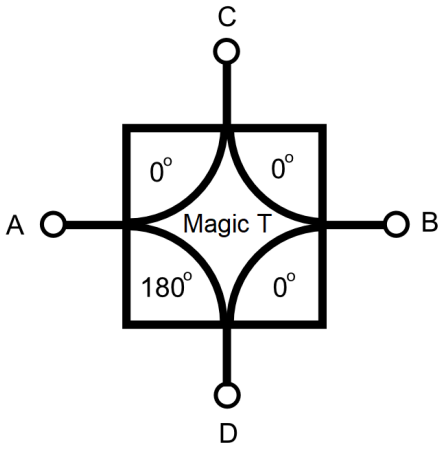

Figure 17: The schematic of the *180°-RF hybrid* circuit. The device splits the incoming signal at port A into two parts. At ports C and D, signals of equal intensity but opposite phase are generated. The sum of the signals reflected from these ports appears at port B.

If the input is at port A, with a 50 Ω termination at port D and the probe at port C, then the signal reflected from the probe appears at port B, subtracted from the ideally reflected signal of port D. The probe is matched to 50 Ω when the reflected signal is close to zero.

4 Proceeding with the measurement

4.1 Tuning the measuring circuit

The measuring circuit is tuned using a swept spectrum analyzer (SignalHound) and a so-called "Magic Tee". This includes a signal source (*tracking generator*), the frequency of which changes uniformly over time. The signal is measured by a heterodyne spectrum analyzer, which we operate using the factory software `Spike.exe`. After starting the program, select the `Scalar Network Analysis` option under `Analysis mode`.

During the laboratory exercise, the NMR probes need to be tuned to 50 Ω at the Larmor frequency determined by the nuclei. The sample will be placed inside the coil, and this coil will be used to generate the excitation pulses as well as to detect the signal by measuring the voltage induced within it.

One input of the Magic T is connected to the tracking generator, we also connect our circuit and a 50 Ω termination (which has an impedance of exactly 50 Ω). At the output, the difference between the signals arriving from both sides will appear, which is obviously minimal when the impedance of our circuit is exactly 50 Ω. This signal is then fed into the input of the spectrum analyzer.

When examining the signal on the spectrum analyzer, we need to adjust both capacitors so that at the NMR operating frequency, the reflected signal from the circuit is minimized (approximately $10 - 20$ dB lower than the reflection far from the resonance).

4.2 Measuring program and signal processing

At the end of the lab, students will use a pre-prepared probe head with the 300 MHz NMR device available on-site to try out various pulse sequences using the TECMAG spectrometer. The interface and the most important commands of the measurement program are shown in the appendix. The output files of the device can be directly opened with the Origin program installed on the measuring computer, but they can also be exported as `.txt` files or processed in

Python using the `nmrglue` package. If preferred, the conversion to `.txt` format should be carried out during the lab session!

Basic pulse sequences: Prior to the lab, the most important pulse sequences were created as a reference. However, the goal of the lab exercise is also for students to creatively program their own pulse sequences based on a simple example and freely test them.
The pulse sequences created are:

`FID_no_phase`:	FID.
`FID_no_phase_full_pulse`:	pulses and FID also visible, no phase cycling.
`FID_phase_cyc`:	FID with phase cycling.
`ECHO_full_pulse`:	pulses and the full ECHO.
`ECHO_phase_cyc`:	ECHO with phase cycling.
`CP_full_pulse`:	CP pulse sequence with all the pulses.
`CPMG`:	CPMG pulse sequence with artefact (parasite) FIDs.
`Inversion_recovery`:	sequence for measuring T_1.

5 Preparation exercises for the laboratory practice

These tasks should be completed before the laboratory practice! (*In parentheses, we describe the tasks expected in the report. We do not require a theoretical introduction in the lab report.*)

1. Prepare a program (in Excel, Maple, Python, etc.) that calculates the self-inductance coefficient from the dimensions of a solenoid coil. (*Expected result: the short code and calculation result, e.g., for a coil with 10 turns, 10 mm in length, and 5 mm in diameter.*)

2. Prepare a similar program that, given input parameters R, L, C_1, and C_2, determines the real and imaginary parts of the impedance $Z(\omega)$ as a function of frequency for both circuits in Figure 16. For example, with $R = 1\ \Omega$, $L = 1\ \mu$H, $C_1 = 100$ pF, and $C_2 = 10$ pF, find visually the frequency where the impedance of the circuit is real 50 Ω. Plot the imaginary part of the reflection coefficient $\Gamma = \frac{Z(\omega)-Z_0}{Z(\omega)+Z_0}$ (where $Z_0 = 50\ \Omega$) as a function of its real part (this is known as the Smith chart) and interpret the results! (*Expected result: The Smith chart with the above data.*)

3. For an operating frequency of 80 MHz with $L = 0.5\ \mu$H and $R = 1\ \Omega$, determine the values of C_T and C_M for the circuit on the left side of Figure 16 for optimal tuning! Similarly, for an operating frequency of 300 MHz with $L = 0.1\ \mu$H and $R = 1\ \Omega$, determine the values of C_T and C_M for the circuit on the right side of Figure 16 for optimal tuning! (*Expected result: The capacitance values for both cases.*)

4. Find data for the proton T_1 and T_2 relaxation times in water in literature. (*Expected result: The relaxation times with references.*)

6 Lab exercises

1. Write a report based on the measurement description and the preparation tasks. With the help of the measurement instructor, identify the main components of the NMR equipment.

2. Using the Hybrid Tee, first find the frequency corresponding to the smallest reflection from the measurement head. Tune the circuit to a 50 Ω impedance at the 300 MHz Larmor frequency used for measurement by adjusting the C_T and C_M capacitors. (*Expected result: Screenshot of the observed curve when optimally matched and tuned.*)

3. Try to observe FID with a pulse (`FID_no_phase`). In RS mode, "play" with the sequence parameters: frequency, phase, pulse length, receiver gain, etc., and understand the role of these parameters. Determine the precise Larmor frequency using the Fourier transform of the FID. (*Expected result: The FID FT graphically and the value of the Larmor frequency.*)

4. Record the FID signal again with and without phase cycling, and demonstrate the effect of phase cycling on the FT spectra. (Phase cycling can be accessed by clicking on the pulse phase parameter, e.g., `F1_ph`.) Suggestion: The expected result is best observed when the LO frequency is detuned by approximately 500-1000 Hz from the Larmor frequency and possibly using a slightly higher *receiver gain.* (*Expected result: The FID FT with and without phase cycling.*)

5. Following this, create a spin-echo sequence, starting from the already programmed FID! (If you encounter difficulties, use `ECHO_full_pulse` and then optimize the two pulse lengths.) Modify this to include phase-cycling as described in the notes! Measure with the sequences and interpret the results. (*Expected result: Time-domain and frequency-domain spin-echo with and without phase cycling, and the optimal pulse lengths.*)

6. Examine the Carr-Purcell pulse sequence and the Carr-Purcell-Meiboom-Gill pulse sequence! Use the (`CP_full_pulse`, `CPMG_full_pulse`) pulse sequences. Show that by adjusting the optimal pulse length, the CPMG pulse sequence is less sensitive to changes in pulse length compared to the CP sequence! (*Expected result: Signals obtained with CP and CPMG pulse sequences for optimal and adjusted pulse lengths, with 4 time-domain measurements*) Optional task: Modify the CP pulse sequence based on the notes to correct for accumulated phase errors! (Hint: use the 1/2D dimension described in the appendix.)

7. Determine the T_2 spin-spin relaxation time from the CPMG measured at the optimal pulse length. Compare this to the known literature value for water. (*Expected result: Evaluation of T_2 and comparison with literature values.*)

8. Create a pulse sequence to measure the T_1, spin-lattice relaxation time and perform the measurement (`Inversion_recovery`). Compare the relaxation time with literature data! (*Expected result: Example of a time-domain measurement used for determining T_1, and comparison of the measured T_1 value with literature data.*)

7 Appendix

7.1 TNMR software user interface

The TNMR interface used for the measurement is shown in Figure 18. In the window marked with red, the pulse sequence can be set. If the window is not open, it can be accessed via the icon marked with a red frame in the toolbar. The most important parameters of the pulse sequence are described in section 7.2. The values of these parameters can be adjusted either in the aforementioned window or in the parameter list enclosed in a blue window. The measurement results are displayed in the window outlined in green. It is important to note that when saving, the currently displayed data will be saved along with the parameters of the pulse sequence.

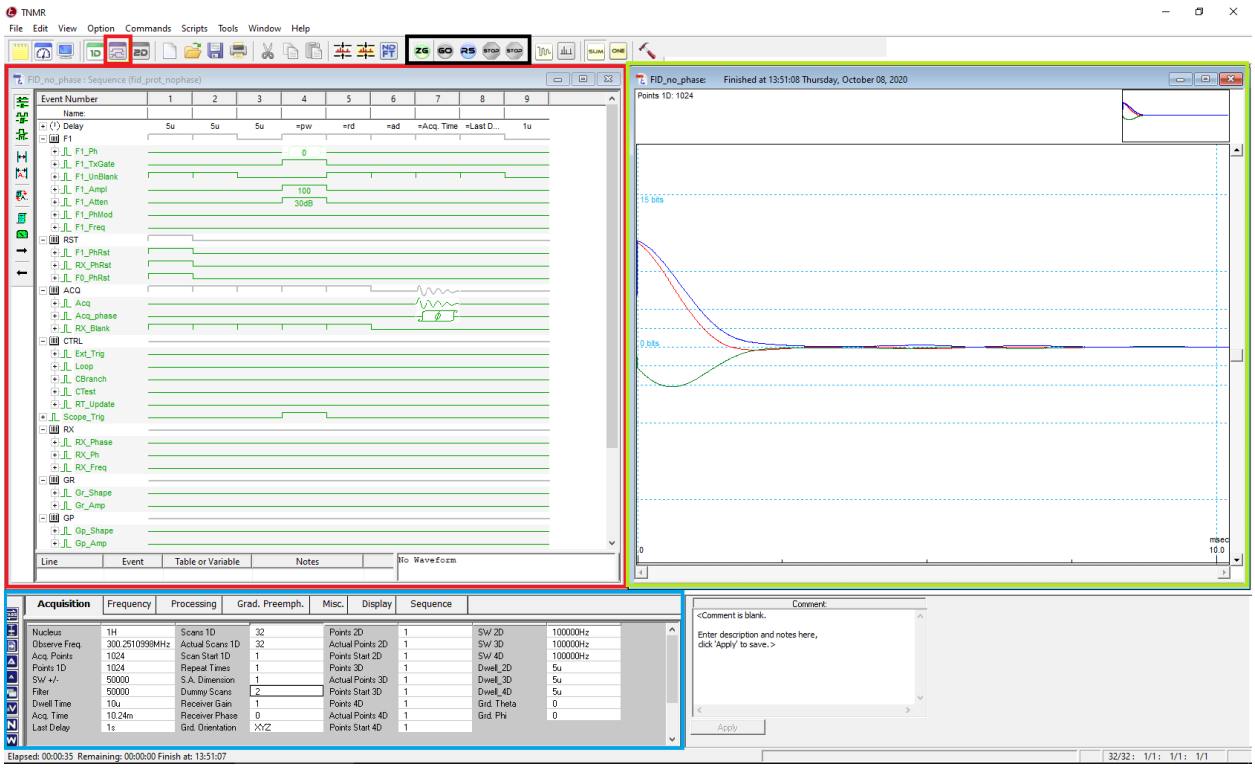

Figure 18: The TNMR user interface.

The icons framed in black are used to start and stop the measurement. There are three different ways to start a measurement. The first is called *zero go* (`ZG`), which always starts the set sequence from the beginning while clearing the previous data from the buffer. The second option is the so-called *go* (`GO`), which either starts the measurement as

in the previous option or resumes a paused measurement if possible. The last option is the *repeat scan* (`RS`), which starts the set sequence but only displays the most recent measurement. This measurement will continue until stopped with the `stop` button. With the two icons located to the right of these, we can switch between the time domain and frequency domain; however, switching only works during ZG measurements, not during RS.

During a measurement started in `RS` mode, there is an option to adjust the parameters in real time. This is useful, for example, when you want to optimize the pulse length. This can be done in the window that can be opened with the button outlined in red on the left side on Figure 19. Only the parameter currently selected in the parameter list can be adjusted. The `coarse` button adjusts the parameter value by the set `step size`, while the `fine` button adjusts it by one-tenth of the `step size`. It is recommended to select the parameter you want to tune and set the `step size` before starting the measurement.

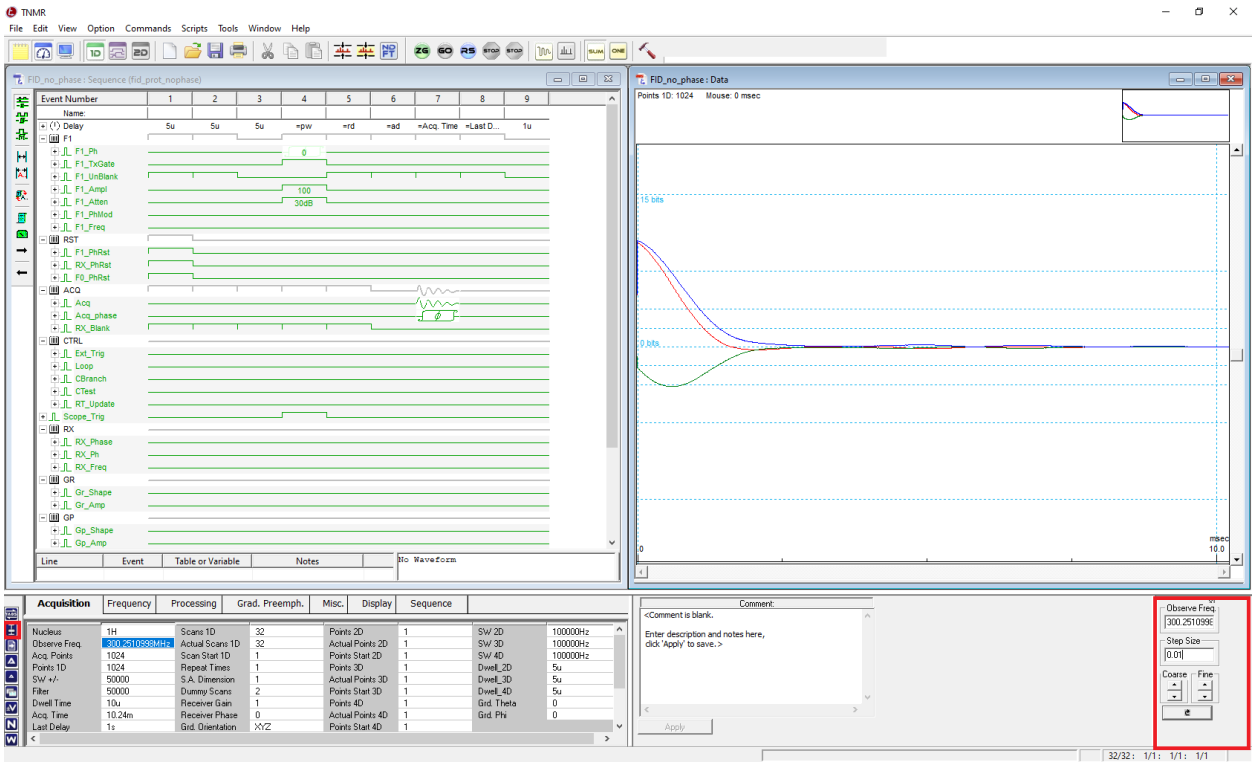

Figure 19: The TNMR interface for adjusting parameters in `RS` mode.

7.2 The most important parameters in TNMR

`Observe Freq.`	Frequency of local oscillator
`Acq. Points`	Number of measurement points
`SW /-+`	Spectral Width in Hz
`Acq. Time`	Length of the measurement (not adjustable)
`Last Delay`	Waiting time between pulse sequences
`Scans 1D`	Number of measurements in one take
`Receiver Gain`	Input amplification in ADC

7.3 Usage of multidimensional tables

The TNMR program provides the option for so-called multidimensional measurements. This essentially involves varying different parameters of the pulse sequences in nested loops. The placement of the various panels is shown in Figure 20 with red outlines. In the `F1_Ph` section, the phase of the pulses can be adjusted, and in the `Delay` section, the duration of individual pulses or time intervals can be changed, with the option to incrementally modify them, as seen in the open window in the image. To use multidimensional measurements, the number of scans (e.g., 2D, 3D, etc.) must be specified in the third column of the `Acquisition` parameters, and navigation between these can be done in the section outlined in blue. The section outlined in green contains the `Loop` channel, which repeats selected parts of the sequence during an iteration, a feature that can be advantageously used mainly for 1/2D measurements.

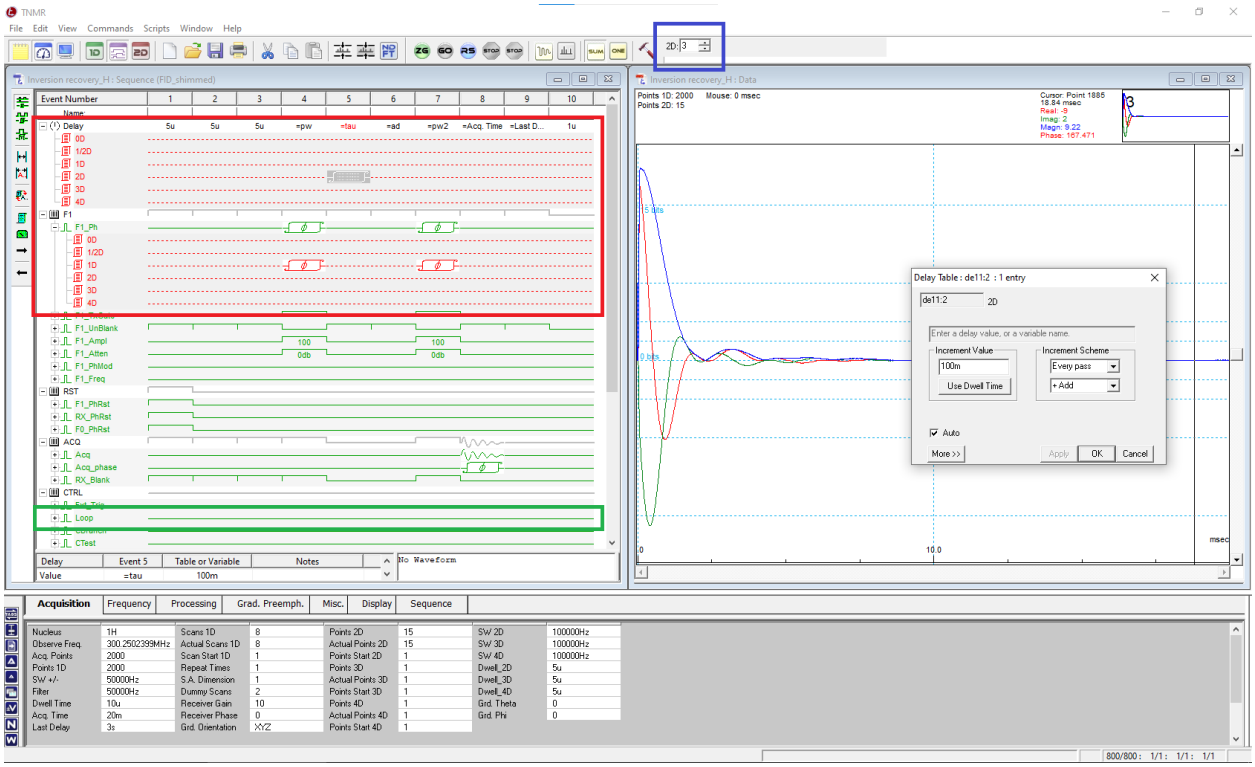

Figure 20: Displaying multidimensional sequence tables, for example the `F1\_Ph\` channel. It appears after expanding the channel with the + symbol.

The 1/2D corresponds to the variation of the parameters of consecutive pulses in a given pulse sequence (most commonly used for CP correction). The 1D refers to the averaging between individual pulse sequences, where phase cycling most commonly appears. The 2D can be used, for example, when measuring T_1, where the waiting time after the inversion pulse is placed into the 2D array (while averaging each measurement according to the 1D array). Higher dimensions like 3D or 4D can also be used when we want to vary additional parameters in a nested manner.

7.4 Description of 1/2-dimension

As in the multi-dimensional cases, in half-dimension (1/2D) nested loops are repeated, but within the 1D. Since 1D is the base sequence of the program, if we include any 1/2D pulse, the pulse phase would not change. For this, we use `Loop`, which repeats the selected part for n iterations within each 1D measurement. If the loop is started on a 1D table, the table sequence steps in phase and scans, and in the next 1D iteration, it starts the sequence as if continuing from the previous one.

The 1/2D table steps the sequences similarly, but its peculiarity is that in the next 1D iteration, it "resets" the stepping position, meaning it does not continue where it left off but starts from the beginning. So, the difference is, that in 1D, the loop places a dynamic flag at the last phase, while in 1/2D, it places a fixed flag at the initial phase, which determines the next's start. Thus, in 1D, the next sampling can start from the middle of the pulse sequence if the sequence lengths are not integer multiples of n. Utilizing this, it is possible to create a sequence that compensates for CP rotations in X, counteracting the appearance of parasitic voltages, and each echo is in the same direction:

$$\begin{aligned} \Phi_1 &= \quad 0\ 2 \\ \Phi_2 &= \quad 0\ 2 \\ \Phi_{31} &= \quad 0\ 2 \end{aligned}$$

In this sequence, Φ_2 and Φ_{31} are located within the loop, with Φ_2 implemented as a 1/2D table. This means that there will be n acquisition within a single 1D iteration, with the phase changing according to Φ_{31}. However, the effectiveness of our measurement is also influenced by the choice of n. If n is odd, the individual echoes will appear clearly, from whose envelope we can derive T_2; however, if the loop number is even, we get a significantly different result, due to the behaviour of the loop described earlier.

It is worth paying attention to the fact that if we observe a doubling of the signal in our sampling, a slight time delay should be inserted within the loop. This error may occur because the program cannot properly reset to the beginning of the cycle, which disrupts the memory management.

7.5 Numerical solutions for the preparation tasks

The values can be obtained both numerically and analytically. For the lower frequency circuit (left-hand side of Figure 16), at a working frequency of 80 MHz, with $L = 0.5$ μH and $R = 1$ Ω, the optimal tuning results are $C_{\mathrm{T}} = 6.8$ pF and $C_{\mathrm{M}} = 1.12$ pF.

The analytical expressions are:

$$C_{\mathrm{T}} = (Z_0 - R)\, C_{\mathrm{M}}\, ()^{-1} \tag{2}$$

Similarly, for the right-hand side circuit of Figure 16, at a working frequency of 300 MHz, with $L = 0.1$ μH and $R = 1$ Ω, the optimal tuning results are $C_{\mathrm{T}} = 2.92$ pF and $C_{\mathrm{M}} = 74.27$ pF.

$$C_{\mathrm{T}} = ()^{-1}\, C_{\mathrm{M}}\, ()^{-1} \tag{3}$$